

[Ni(Et₂PCH₂NMeCH₂PEt₂)₂]²⁺ as a Functional Model for Hydrogenases

Calvin J. Curtis, Alex Miedaner, Rebecca Ciancanelli, William W. Ellis, Bruce C. Noll, M. Rakowski DuBois, and Daniel L. DuBois*

National Renewable Energy Laboratory, 1617 Cole Boulevard, Golden, Colorado 80401-3393, and the Department of Chemistry and Biochemistry, University of Colorado, Boulder, Colorado 80309

Received October 8, 2002

The reaction of Et₂PCH₂N(Me)CH₂PEt₂ (PNP) with [Ni(CH₃CN)₆](BF₄)₂ results in the formation of [Ni(PNP)₂](BF₄)₂, which possesses both hydride- and proton-acceptor sites. This complex is an electrocatalyst for the oxidation of hydrogen to protons, and stoichiometric reaction with hydrogen forms [HNi(PNP)(PNHP)](BF₄)₂, in which a hydride ligand is bound to Ni and a proton is bound to a pendant N atom of one PNP ligand. The free energy associated with this reaction has been calculated to be -5 kcal/mol using a thermodynamic cycle. The hydride ligand and the NH proton undergo rapid intramolecular exchange with each other and intermolecular exchange with protons in solution. [HNi(PNP)(PNHP)](BF₄)₂ undergoes reversible deprotonation to form [HNi(PNP)₂](BF₄) in acetonitrile solutions (pK_a = 10.6). A convenient synthetic route to the PF₆⁻ salt of this hydride involves the reaction of PNP with Ni(COD)₂ to form Ni(PNP)₂, followed by protonation with NH₄PF₆. A pK_a of value of 22.2 was measured for this hydride. This value, together with the half-wave potentials of [Ni(PNP)₂](BF₄)₂, was used to calculate homolytic and heterolytic Ni-H bond dissociation free energies of 55 and 66 kcal/mol, respectively, for [HNi(PNP)₂](PF₆). Oxidation of [HNi(PNP)₂](PF₆) has been studied by cyclic voltammetry, and the results are consistent with a rapid migration of the proton from the Ni atom of the resulting [HNi(PNP)₂]²⁺ cation to the N atom to form [Ni(PNP)(PNHP)]²⁺. Estimates of the pK_a values of the NiH and NH protons of these two isomers indicate that proton migration from Ni to N should be favorable by 1–2 pK_a units. Cyclic voltammetry and proton exchange studies of [HNi(depp)₂](PF₆) (where depp is Et₂PCH₂CH₂CH₂PEt₂) are also presented as control experiments that support the important role of the bridging N atom of the PNP ligand in the proton exchange reactions observed for the various Ni complexes containing the PNP ligand. Similarly, structural studies of [Ni(PNBuP)₂](BF₄)₂ and [Ni(PNP)(dmpm)](BF₄)₂ (where PNBuP is Et₂PCH₂N(Bu)CH₂PEt₂ and dmpm is Me₂PCH₂PMe₂) illustrate the importance of tetrahedral distortions about Ni in determining the hydride acceptor ability of Ni(II) complexes.

Introduction

Hydrogenase enzymes catalyze the oxidation of hydrogen or its reverse: the reduction of protons to hydrogen. This reaction is of interest because of its role in biological metabolic processes and its potential importance to fuel cells. From a fundamental perspective, this is the simplest electrochemical reaction involving bond formation or cleavage. Two well-established classes of hydrogenases are the Fe-only and the NiFe hydrogenases. Recent structural studies of the Fe-only hydrogenase from *Desulfovibrio desulfuricans* suggest that the site for hydrogen activation contains two Fe atoms bridged by a di(thiomethyl)amine ligand, HN(CH₂S⁻)₂.^{1–4} In the reduced form, one iron is bound to

two terminal CO ligands and one cyanide ligand with a vacant coordination site adjacent to the di(thiomethyl)amine ligand. The nitrogen atom of this ligand is thought to play an important role in the heterolytic cleavage of hydrogen at the active site and in the transfer of the protons from the active site to the exterior of the enzyme via a proton-transfer pathway.^{1,5}

These results have led to model studies of Fe dimers containing propane dithiolate and CH₃N(CH₂S)₂ bridges.^{6–9}

- (1) Nicolet, Y.; de Lacey, A. L.; Vernède, X.; Fernandez, V. M.; Hatchikian, E. C.; Fontecilla-Camps, J. C. *J. Am. Chem. Soc.* **2001**, *123*, 1596–1601.
- (2) Peters, J. W.; Lanzilotta, W. N.; Lemon, B. J.; Seefeldt, L. C. *Science* **1998**, *282*, 1853–1858.
- (3) Pereira, A. S.; Tavares, P.; Moura, I.; Moura, J. J. G.; Huynh, B. H. *J. Am. Chem. Soc.* **2001**, *123*, 2771–2782.
- (4) Peters, J. W. *Curr. Opin. Struct. Biol.* **1999**, *9*, 670–676.
- (5) Fan, H.-J.; Hall, M. B. *J. Am. Chem. Soc.* **2001**, *123*, 3828–3829.

* To whom correspondence should be addressed. E-mail: dan_dubois@nrel.gov.

H/D exchange and hydrogen evolution has been observed for some of these complexes, but evidence is lacking for participation of the nitrogen atom of the bridging dithiolate ligand in these model compounds. However, the proposed interactions between the nitrogen atom of the bridging dithiolate ligand, Fe, and H₂ remain reasonable. Examples of ligand-appended bases interacting with coordinated dihydrogen to produce heterolytic cleavage of hydrogen are known for a number of transition metal complexes.¹⁰ In addition, the closely related phenomenon of hydrogen bonding between metal hydrides and positively charged hydrogen atoms bound to electronegative elements, such as nitrogen or oxygen, has also been studied in some detail.¹¹ These bonds have been shown to have bond energies as large as 5–6 kcal/mol, which would indicate that this type of interaction could be important in enzymatic systems.

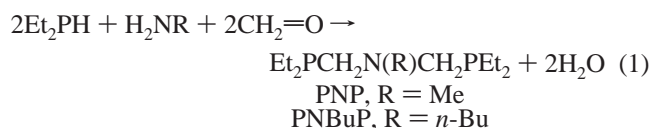
In the NiFe hydrogenases, the Fe atom has an almost identical coordination sphere to that observed for the Fe-only hydrogenase.^{12–14} The Ni atom is bound to four sulfur atoms of cysteine residues. Two of these sulfurs bridge the Fe and Ni atoms. The four sulfur atoms coordinated to Ni exhibit a large distortion from the ideal positions expected for either a tetrahedral or square planar geometry. Various roles have been proposed for the Fe and Ni atoms in the activation/production of hydrogen on the basis of spectroscopic and theoretical studies.^{15–18} Whatever their roles, it is likely that they act in concert because the sulfur bridges should provide strong electronic coupling between the two metals.

In previous studies, we have used the heterolytic cleavage of hydrogen by [Ni(diphosphine)₂]²⁺ complexes in the presence of an amine base to determine the hydricity of the corresponding [HNi(diphosphine)₂]⁺ complexes.¹⁹ In this paper, we describe the preparation of [Ni(diphosphine)₂]²⁺ complexes containing ligand-appended nitrogen bases. It

has been found that [Ni(Et₂PCH₂NMeCH₂PEt₂)₂]²⁺, [Ni(PNP)₂]²⁺, catalyzes the electrochemical oxidation of hydrogen and reacts stoichiometrically with hydrogen to form complexes in which the hydride ligand is associated with nickel and the proton is bound by nitrogen. Rapid exchange occurs between these two sites. This complex also readily exchanges both the hydride ligand and the proton on nitrogen with protons in solution. Deprotonation of this complex leads to the formation of [HNi(PNP)₂]⁺. Electrochemical studies of the latter complex are consistent with a rapid and reversible transfer of a proton between the metal and the nitrogen atom of the PNP ligand as the Ni complex is oxidized and reduced. The observed catalysis, the heterolytic activation of hydrogen, and the transfer of protons between Ni and N suggest that [Ni(PNP)₂]²⁺ is a good functional model of the Fe-only hydrogenases.

Results

Syntheses and Reactions. The ligand Et₂PCH₂NMeCH₂PEt₂ (PNP) was prepared by the reaction of 2 equiv of diethylphosphine and formaldehyde with 1 equiv of methylamine in the form of the hydrochloride salt, as shown in reaction 1. This Manich-type reaction has been used extensively for the preparation of a variety of mixed phosphine–amine ligands with methylene bridges.²⁰ The ligand PNBP was prepared in an analogous fashion. The NMR spectral data and analytical data are consistent with the assigned structure (see Experimental Section for details).



Ni(II) Complexes. Reaction of 2 equiv of PNP with [Ni(CH₃CN)₆](BF₄)₂ in acetonitrile results in the formation of red [Ni(PNP)₂](BF₄)₂. Solutions of this complex bleach immediately on exposure to air, and [Ni(PNP)₂](BF₄)₂ is significantly more air-sensitive than both its hydride and Ni(0) analogues described in following paragraphs. The spectral data and electrochemical data for this complex are consistent with its formulation (see Experimental Section).

The chemical properties of [Ni(PNP)₂](BF₄)₂ and [Ni(PNBP)₂](BF₄)₂ and their derivatives are identical with respect to the chemistry described in this paper with the exception that X-ray quality crystals were obtained for [Ni(PNBP)₂](BF₄)₂. Crystallization of [Ni(PNBP)₂](BF₄)₂ from a dichloromethane/ethanol mixture resulted in red crystals and a yellow powder. A ³¹P NMR spectrum of this mixture indicated the presence of both [Ni(PNBP)₂](BF₄)₂ (red) and [HNi(PNBP)₂](BF₄) (yellow). The latter is produced by the oxidation of ethanol, as verified by addition of ethanol to an NMR sample of [Ni(PNBP)₂](BF₄)₂ in CD₃CN. An X-ray diffraction study of the red crystals confirmed their assignment to [Ni(PNBP)₂](BF₄)₂. A per-

- (6) Lyon, E. J.; Georgakaki, I. P.; Reibenspies, J. H.; Darensbourg, M. Y. *J. Am. Chem. Soc.* **2001**, *123*, 3268–3278.
- (7) Zhao, X.; Georgakaki, I. P.; Miller, M. L.; Yarbrough, J. C.; Darensbourg, M. Y. *J. Am. Chem. Soc.* **2001**, *123*, 9710–9711.
- (8) Gloaguen, F.; Lawrence, J. D.; Rauchfuss, T. B. *J. Am. Chem. Soc.* **2001**, *123*, 9476–9477.
- (9) Lawrence, J. D.; Li, H.; Rauchfuss, T. B.; Bénard, M.; Rohmer, M.-M. *Angew. Chem., Int. Ed.* **2001**, *40*, 1768–1771.
- (10) Lee, D.-H.; Patel, B. P.; Clot, E.; Eisenstein, O.; Crabtree, R. H. *Chem. Commun.* **1999**, 297–298. Chu, H. S.; Lau, C. P.; Wong, K. Y.; Wong, W. T. *Organometallics*, **1998**, *17*, 2768. Laugh, A. J.; Park, S.; Ramachandran, R.; Morris, R. H. *J. Am. Chem. Soc.* **1994**, *116*, 8356–8357.
- (11) Custelcean, R.; Jackson, J. E. *Chem. Rev.* **2001**, *101*, 1963–1980.
- (12) Volbeda, A.; Garcin, E.; Piras, C.; de Lacey, A. L.; Fernandez, V. M.; Hatchikian, E. C.; Frey, M.; Fontecilla-Camps, J. C. *J. Am. Chem. Soc.* **1996**, *118*, 12989–12996.
- (13) Higuchi, Y.; Ogata, H.; Miki, K.; Yasuoka, N.; Yagi, T. *Structure* **1999**, *7*, 549–556.
- (14) Garcin, E.; Vernede, X.; Hatchikian, E. C.; Volbeda, A.; Frey, M.; Fontecilla-Camps, J. C. *Structure* **1999**, *7*, 557–565.
- (15) Amara, P.; Volbeda, A.; Fontecilla-Camps, J. C.; Field, M. J. *J. Am. Chem. Soc.* **1999**, *121*, 4468–4477.
- (16) Pavlov, M.; Siegbahn, P. E. M.; Blomberg, M. R. A.; Crabtree, R. H. *J. Am. Chem. Soc.* **1998**, *120*, 548–555.
- (17) Niu, S.; Thomson, L. M.; Hall, M. B. *J. Am. Chem. Soc.* **1999**, *121*, 4000–4007.
- (18) Stein, M.; van Lenthe, E.; Baerends, E. J.; Lubitz W. *J. Am. Chem. Soc.* **2001**, *123*, 5839–5840.
- (19) Curtis, C. J.; Miedaner, A.; Ellis, W. W.; DuBois, D. L. *J. Am. Chem. Soc.* **2002**, *124*, 1918–1925.

- (20) Moedritzer, K.; Irani, R. R. *J. Org. Chem.* **1966**, *31*, 1603–1607. Matienzo, L. J.; Grim, S. O. In *Inorganic Synthesis*; Basolo, F., Ed.; McGraw-Hill: New York, 1976; Vol. 16, pp 198–199.

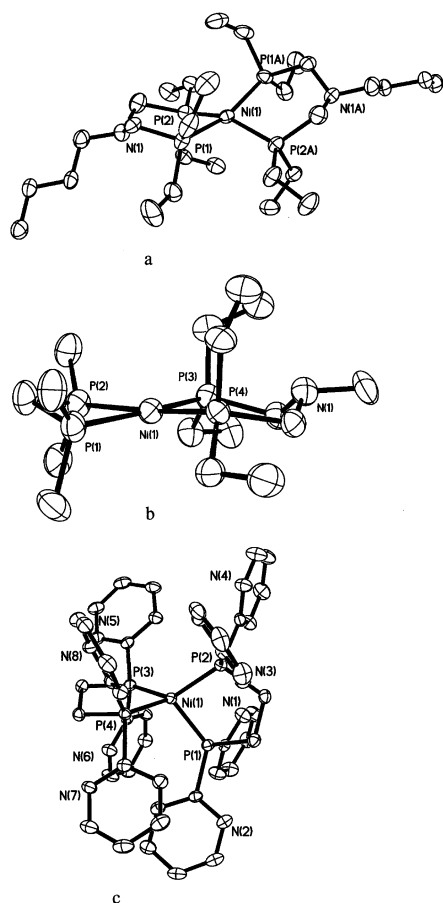


Figure 1. Drawings of (a) $[\text{Ni}(\text{PNBuP})_2]^{2+}$, (b) $[\text{Ni}(\text{PNP})(\text{dmpm})]^{2+}$, and (c) $\text{Ni}(\text{dpype})_2$ indicating atom numbering schemes. Thermal ellipsoids are drawn at 50% probability.

Table 1. Selected Bond Distances (Å)

compd	Ni–P(1)	Ni–P(2)	Ni–P(3)	Ni–P(4)
$[\text{Ni}(\text{PNBuP})_2](\text{BF}_4)_2$	2.2304(9)	2.2371(8)		
$[\text{Ni}(\text{PNP})(\text{dmpm})](\text{BF}_4)_2$	2.2276(16)	2.235(2)	2.1889(15)	2.1876(15)
$\text{Ni}(\text{dpype})_2$	2.1483(9)	2.1526(7)	2.1478(7)	2.1461(7)

Table 2. Selected Bond Angles (deg)

$[\text{Ni}(\text{PNBuP})_2](\text{BF}_4)_2$			
P(1)–Ni–P(2)	89.66(3)	P(1A)–Ni–P(2)	95.07(3)
P(1)–Ni–P(1A)	159.50(6)	P(1A)–Ni–P(2A)	89.66(3)
P(1)–Ni–P(2A)	95.07(3)	P(2)–Ni–P(2A)	153.21(6)
$[\text{Ni}(\text{PNP})(\text{dmpm})](\text{BF}_4)_2$			
P(1)–Ni–P(2)	73.84(7)	P(2)–Ni–P(3)	95.72(7)
P(1)–Ni–P(3)	169.54(6)	P(2)–Ni–P(4)	168.48(7)
P(1)–Ni–P(4)	96.21(6)	P(3)–Ni–P(4)	94.24(6)
$\text{Ni}(\text{dpype})_2$			
P(1)–Ni–P(2)	90.59(3)	P(2)–Ni–P(3)	131.32(3)
P(1)–Ni–P(3)	114.47(3)	P(2)–Ni–P(4)	116.78(3)
P(1)–Ni–P(4)	114.06(3)	P(3)–Ni–P(4)	91.23(3)

spective drawing of the $[\text{Ni}(\text{PNBuP})_2]^{2+}$ cation is shown in Figure 1a. Table 1 contains selected bond lengths for this complex, and Table 2 contains selected bond angles. It can be seen from Figure 1a that the $[\text{Ni}(\text{PNBuP})_2]^{2+}$ cation is best described as a tetrahedrally distorted square planar complex. The tetrahedral distortion, as measured by the dihedral angle between the two planes defined by the two phosphorus atoms of each chelating diphosphine ligand and

Ni, is 34.1° , which indicates a tetrahedral distortion approximately one-third of the way between a square planar geometry and a tetrahedron. This large tetrahedral distortion can be attributed to steric interactions between the ethyl substituents on the two different diphosphine ligands, but it may have an electronic component as well.²¹ The P–Ni–P bond angle of 89.7° for the diphosphine ligands is similar to that observed for the analogous $[\text{Ni}(\text{dmpm})]^{2+}$ cation (91.5°), and the Ni–P bond lengths (2.23 Å average) are normal for Ni^{2+} phosphine complexes.^{21,22} The six-membered ring formed by Ni and the PNBuP ligand is in the chair form and exhibits some disorder, consistent with the expected conformational lability.

$[\text{Ni}(\text{PNP})(\text{dmpm})](\text{BF}_4)_2$ (where dmpm is bis(dimethylphosphino)methane) can be prepared by addition of $[\text{Ni}(\text{CH}_3\text{CN})_6](\text{BF}_4)_2$ to a 1:1 mixture of the two ligands in acetonitrile. The ^{31}P NMR spectrum of this complex, which has an AA'XX' spin system, consists of two apparent doublets at 2.25 and -53.42 ppm in CD_3CN . These chemical shift values are in the ranges expected for phosphorus atoms in six- and four-membered rings on Ni.²³ Crystallization of this complex from a mixture of dichloromethane and ethanol produced crystals suitable for an X-ray diffraction study. A perspective drawing of the $[\text{Ni}(\text{PNP})(\text{dmpm})]^{2+}$ cation is shown in Figure 1b. Tables 1 and 2 contain selected bond lengths and bond angles, respectively, for this complex. It can be seen from Figure 1b that the $[\text{Ni}(\text{PNP})(\text{dmpm})]^{2+}$ cation is almost strictly planar with a dihedral angle between the two planes defined by the two phosphorus atoms of each chelating diphosphine ligand and Ni of 5.9° . This is much smaller than the 34.1° angle observed for $[\text{Ni}(\text{PNBuP})_2](\text{BF}_4)_2$. The P–Ni–P bond angles of the two diphosphine ligands are quite different for the two ligands: 94.2° for PNP and 73.8° for dmpm. The Ni–P bond lengths are again in the normal range expected for a Ni^{2+} complex (2.21 Å average).^{21,22}

In contrast to the PNP and PNBuP, addition of $[\text{Ni}(\text{CH}_3\text{CN})_6](\text{BF}_4)_2$ to acetonitrile solutions of dpype (where dpype is bis(di-2-pyridylphosphino)ethane)²⁴ produced a paramagnetic product(s), as indicated by very broad ^1H NMR resonances and no observable ^{31}P NMR resonances. The desired square planar Ni(II) complex with four coordinated phosphorus atoms should be diamagnetic. Similar results were obtained when $\text{Ni}(\text{dpype})_2$, described in the following paragraph, was oxidized with ferrocenium hexafluorophosphate.

Ni(0) Complexes. $\text{Ni}(\text{COD})_2$ (where COD is 1,5-cyclooctadiene) reacts with 2 equiv of PNP to form $\text{Ni}(\text{PNP})_2$, **2** (reaction 2, step 1). The ^1H and ^{31}P NMR spectral data, elemental analysis, and electrochemical data of white $\text{Ni}(\text{PNP})_2$ are all consistent with its formulation (see Experimental Section). Similarly, reaction of 2 equiv of 1,2-bis-

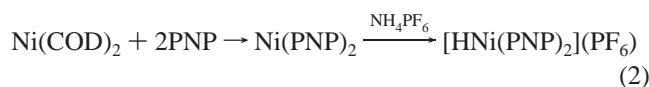
(21) Miedaner, A.; Haltiwanger, R. C.; DuBois, D. L. *Inorg. Chem.* **1991**, *30*, 417–427.

(22) Berning, D. E.; Noll, B. C.; DuBois, D. L. *J. Am. Chem. Soc.* **1999**, *121*, 11432–11447.

(23) Garrou, P. E. *Chem. Rev.* **1981**, *81*, 229–266.

(24) Bowen, R. J.; Garner, A. C.; Berners-Price, S. J.; Jenkins, I. D.; Sue, R. E. *J. Organomet. Chem.* **1998**, *554*, 181–184.

(di-2-pyridylphosphino)ethane (dpype) with Ni(COD)₂ produces Ni(dpype)₂. The spectroscopic, analytic, and X-ray diffraction data for this complex (see Experimental Section) are also consistent with the assigned structure. A perspective drawing of Ni(dpype)₂ is shown in Figure 1c. Tables 1 and 2 contain selected bond lengths and bond angles, respectively, for this complex. It can be seen from Figure 1c that Ni(dpype)₂ is best described as a distorted tetrahedron. The dihedral angle between the two planes defined by the two phosphorus atoms of each chelating diphosphine ligand and Ni is 85.3°. As expected, this angle is much larger than those observed for [Ni(PNP)₂]²⁺ and [Ni(PNP)(dmpm)]²⁺. The average P–Ni–P bond angle formed by Ni and the dpype ligand is 90.9°, which is comparable to those observed for Ni(dppv)₂ (90.7°, where dppv is *cis*-bis(diphenylphosphino)ethylene), and Ni(dedpe)₂ (90.9°, where dedpe is 1-(diethylphosphino)-2-(diphenylphosphino)ethane). The Ni–P bond lengths (2.15 Å average) are in the range expected for a Ni(0) complex and about 0.06 Å shorter than those observed for Ni²⁺ complexes.^{21,22,25}

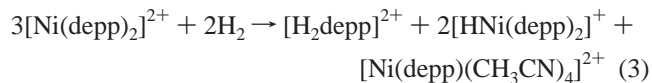


NiH Complexes. The studies described here include results for Ni complexes of both PNP and depp ligands (where depp is 1,3-bis(diethylphosphino)propane), in which the N atom of PNP is replaced by a methylene, CH₂, unit. Comparisons of the hydride complexes of these two ligands help delineate the role of the bridging N atom of the PNP ligand in various reactions described in following paragraphs.

Protonation of Ni(PNP)₂ with ammonium hexafluorophosphate produces [HNi(PNP)₂](PF₆) (reaction 2, step 2). The observation of a resonance at –14.8 ppm in the ¹H NMR spectrum of this complex dissolved in CD₃CN is characteristic of a hydride, and the quintet splitting is consistent with coupling to four phosphorus nuclei. As in the case of [HNi(depp)₂]²⁺ complexes studied previously,¹⁹ the protonation of the Ni(0) complex, Ni(PNP)₂, to form the corresponding hydride complex results in only a small shift (approximately 1 ppm) of the ³¹P NMR resonance. However, ¹H-coupled ³¹P NMR spectra and {³¹P} ¹H NMR spectra confirm coupling between the hydride and phosphorus nuclei. A band at 1933 cm^{–1} in the infrared spectrum is assigned to the Ni–H stretch.

The reaction of [Ni(depp)₂]²⁺ with hydrogen in acetonitrile in the presence of a base such as triethylamine generates [HNi(depp)₂]⁺ and the protonated base, as described previously.¹⁹ In fact, reaction with hydrogen occurs in the absence of base, but in this case, the coordinated diphosphine ligand acts as a base, as shown in reaction 3. Resonances in the ³¹P NMR spectrum are observed in a 1:4 ratio assigned to the protonated diphosphine ligand (a singlet at 19.8 ppm in the ³¹P NMR spectrum with an associated doublet in the ¹H

NMR at 5.93 ppm with ¹J_{PH} = 488 Hz) and the hydride complex, respectively. The assignments for the protonated diphosphine ligand, H₂depp²⁺, were confirmed by an independent synthesis of this compound from depp and HBF₄ in ether. Treatment of the reaction mixture with triethylamine results in the conversion of the protonated diphosphine ligand and [Ni(depp)(CH₃CN)₄]²⁺ into [HNi(depp)₂]⁺.

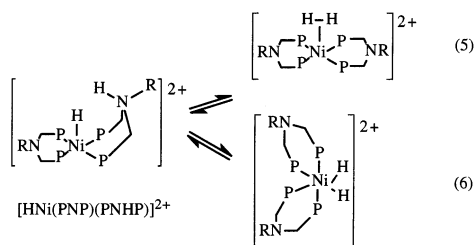


Bubbling hydrogen gas through acetonitrile-*d*₃ and dichloromethane-*d*₂ solutions of [Ni(PNP)₂]²⁺ rapidly bleaches the solutions, and a new hydride species, [HNi(PNHP)(PNP)]²⁺, is formed with a proton bound to the bridging N atom of the diphosphine ligand (reaction 4). In acetonitrile-*d*₃, a new resonance is observed at –3.5 ppm in the ¹H NMR spectrum. When the sample is cooled, this resonance broadens and coalesces, but the low-temperature spectrum cannot be obtained because of the relatively high freezing point of acetonitrile (Figure 1s of Supporting Information). In dichloromethane-*d*₂, the exchange is slower, and the coalesced spectrum is observed at room temperature. When this sample is cooled to –90 °C, two new resonances are observed at –15.2 and 7.4 ppm (Figure 1s). These resonances are assigned to the hydride ligand and NH proton, respectively, of [HNi(PNP)(PNHP)]²⁺. The average of these two chemical shift values, –3.9 ppm, is nearly the same as that observed at room temperature in acetonitrile-*d*₃. Upon warming to room temperature, the original spectrum is obtained. When the sample is heated above room temperature, the complex rapidly decomposes, and no high-temperature spectrum could be obtained in dichloromethane-*d*₂. These spectra indicate that a rapid exchange process occurs in this complex that averages the hydride and the nitrogen-bound proton. The high rate of exchange, approximately 10⁴ s^{–1}, suggests an intramolecular process at the concentrations used for these studies, ~5 × 10^{–3} M. An intermolecular process would require proton transfer at near diffusion-controlled rates. In addition, when [HNi(depp)₂]⁺ and up to 5 equiv of anisidinium (p*K*_a = 11.3)²⁶ or 4-bromoanilinium tetrafluoroborate (p*K*_a = 9.6)²⁶ were dissolved in deuterioacetonitrile, no exchange was observed between the hydride and protonated bases. Slower exchange was probed using 2D ¹H NMR exchange spectroscopy (NOESY), and no exchange was observed on the 1–2 s time scale. Addition of D₂O (0.14 mmol) to a sample of [HNi(depp)₂]⁺ (0.029 mmol) and anisidinium (0.047 mmol) in CD₃CN gave about 20% deuterium incorporation into the NiH site in 18 h, demonstrating relatively slow H/D exchange on a longer time scale. All of this evidence indicates that intermolecular exchange between NiH and NH sites in solution is slow, and the fast exchange observed for [HNi(PNHP)(PNP)]²⁺

(25) Berning, D. E.; Miedaner, A.; Curtis, C. J.; Noll, B. C.; Rakowski DuBois, M. C.; DuBois, D. L. *Organometallics* **2001**, *20*, 1832–1839.

(26) Edidin, R. T.; Sullivan, J. M.; Norton, J. R. *J. Am. Chem. Soc.* **1987**, *109*, 3945–3953.

must be intramolecular. The rapid exchange observed for $[\text{HNi}(\text{PNP})(\text{PNHP})]^{2+}$ is consistent with an intermediate dihydrogen complex (reaction 5) or a Ni^{IV} dihydride complex (reaction 6) that are not observed. Precedent exists for both pathways.^{10,27}



Intermolecular Proton Exchange and Protonation/Deprotonation Reactions. The rapid disappearance (less than 5 min) of the hydride resonance at -14.8 ppm upon addition of D_2O to $[\text{HNi}(\text{PNP})_2]^+$ in CD_3CN indicates that deuterium from D_2O exchanges with the hydride ligand. More rapid exchange of the hydride ligand with H_2O (2.9 equivalents) in solution is indicated by NOESY experiments where a strong exchange cross-peak is observed at mixing times as short as 0.1 s. When D_2O is added to $[\text{HNi}(\text{depp})_2]^+$, less than 10% incorporation of deuterium is observed after 48 h. These observations support the importance of the bridging N atom of the diphosphine ligand for the rapid intermolecular proton exchange observed for $[\text{HNi}(\text{PNP})_2]^+$.

Intermolecular exchange of both the hydride and NH protons is also rapid for $[\text{HNi}(\text{PNP})(\text{PNHP})]^{2+}$. Addition of D_2O to a solution of this compound in acetonitrile- d_3 resulted in a complete and immediate disappearance of the resonance at -3.5 ppm. $[\text{HNi}(\text{PNP})(\text{PNHP})]^{2+}$ also reacts with triethylamine at room temperature to produce $[\text{HNi}(\text{PNP})_2]^+$, as indicated by a hydride resonance at -14.8 ppm. Conversely, the acid, 3-cyanoanilinium tetrafluoroborate, protonates $[\text{HNi}(\text{PNP})_2]^+$ in acetonitrile- d_3 , as indicated by the re-appearance of the resonance at -3.5 in the ^1H NMR spectrum. These results confirm that the protonation of the bridging nitrogen of $[\text{HNi}(\text{PNP})_2]^+$ is reversible. When $[\text{HNi}(\text{PNP})_2]^+$ is treated with a slight excess of 4-cyanoanilinium ($\text{p}K_a = 7.6$)²⁶ or 2,4-dichloroanilinium ($\text{p}K_a = 8.0$)²⁶ in acetonitrile, the resonance assigned to the coordinated PNP ligand (5.46 ppm in the ^{31}P NMR spectrum) broadens and shifts to lower field (7.24 ppm). This resonance is attributed to the completely protonated form of the complex, $[\text{HNi}(\text{PNHP})(\text{PNP})]^{2+}$. By measuring the chemical shift of the ^{31}P NMR resonance of the PNP ligand of $[\text{HNi}(\text{PNP})_2]^+$ and using anisidinium as the acid ($\text{p}K_a = 11.3$)²⁶ an equilibrium constant of 0.19 ± 0.03 was determined for $[\text{Ni}(\text{PNHP})(\text{PNP})]^{2+}$ in acetonitrile. This corresponds to a $\text{p}K_a$ value of 10.6 ± 0.1 . Similar studies of reactions of $[\text{Ni}(\text{PNP})(\text{dmpm})]^{2+}$ with protonated anilinium salts gave a $\text{p}K_a$ value of 8.7 ± 0.5 for $[\text{Ni}(\text{PNHP})(\text{dmpm})]^{3+}$ (see Experimental Section for details). Because of its lower positive charge, $[\text{HNi}(\text{PNP})(\text{PNHP})]^{2+}$ is expected to have a higher $\text{p}K_a$ value

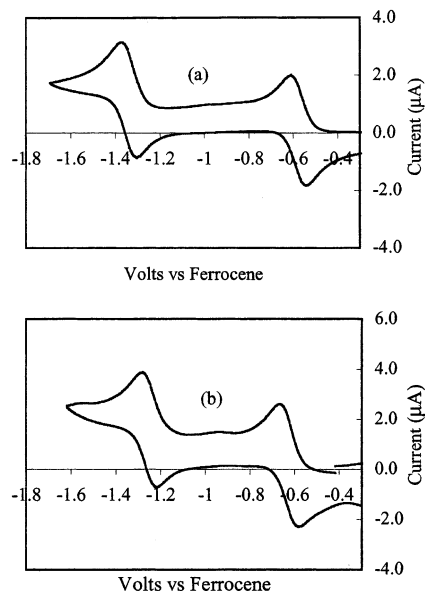


Figure 2. (a) Cyclic voltammogram of a $2.7 \times 10^{-3} \text{ M}$ solution of $[\text{Ni}(\text{depp})_2](\text{BF}_4)_2$ in $0.2 \text{ M NEt}_4\text{BF}_4/\text{CH}_3\text{CN}$. The scan rate is 50 mV/s . (b) Cyclic voltammogram of a $2.1 \times 10^{-3} \text{ M}$ solution of $[\text{Ni}(\text{PNP})_2](\text{BF}_4)_2$ in $0.2 \text{ M NEt}_4\text{BF}_4/\text{CH}_3\text{CN}$. The scan rate is 100 mV/s .

than $[\text{Ni}(\text{PNHP})(\text{dmpm})]^{3+}$. Both values are within the $\text{p}K_a$ range of 7.6–10.6 estimated by Rauchfuss and co-workers for $[\text{Fe}_2\{(\text{SCH}_2)_2\text{N}(\text{H})\text{Me}\}(\text{CO})_6]^+$ in acetonitrile.⁹ Darensbourg and co-workers have reported a $\text{p}K_a$ value between 2.1 and 4.7 in water for the 1,3,5-triaza-7-phosphaadamantane ligand coordinated to $\text{Pt}(0)$.²⁸ This $\text{p}K_a$ range in water corresponds to a range 9.6–12.2 in acetonitrile using a conversion factor of 7.5 for converting aqueous $\text{p}K_a$ values to acetonitrile $\text{p}K_a$ values.²⁹

The $\text{p}K_a$ of $[\text{HNi}(\text{PNP})_2](\text{PF}_6)$ was measured by reaction of $\text{Ni}(\text{PNP})_2$ with $[\text{HPt}(\text{dppe})_2]^+$ (where $\text{dppe} = \text{bis}(\text{diphenylphosphino})\text{ethane}$, $\text{p}K_a = 22.0$) in benzonitrile to form $[\text{HNi}(\text{PNP})_2]^+$ and $\text{Pt}(\text{dppe})_2$. An equilibrium constant of 1.6 was determined for this reaction which corresponds to a $\text{p}K_a$ value of 22.2 in acetonitrile. Previous $\text{p}K_a$ measurements in benzonitrile and acetonitrile have demonstrated that the measured differences in $\text{p}K_a$ values in these solvents are the same.²² This $\text{p}K_a$ value and the $E_{1/2}$ values for the (I/O) and (II/I) couples of $[\text{Ni}(\text{PNP})_2]^{2+}$ in acetonitrile (see later) can be used to calculate the free energies associated with the homolytic and heterolytic Ni–H bond cleavage reactions²² of $[\text{HNi}(\text{PNP})_2]^+$ in acetonitrile of 55 and 66 kcal/mol, respectively. These values are similar to the corresponding values of 54 and 67 kcal/mol reported previously for $[\text{HNi}(\text{depp})_2]^+$.¹⁹

Electrochemical Studies. The cyclic voltammograms of $[\text{Ni}(\text{depp})_2](\text{BF}_4)_2$ and $[\text{Ni}(\text{PNP})_2](\text{BF}_4)_2$ are shown in Figure 2, traces a and b, respectively. Both $[\text{Ni}(\text{depp})_2]^{2+}$ and $[\text{Ni}(\text{PNP})_2]^{2+}$ exhibit two reversible one-electron reductions with ΔE_p values (peak-to-peak potentials) close to 70 mV, the value observed for ferrocene under the same conditions.

(28) Darensbourg, D. J.; Robertson, J. B.; Larkins, D. L.; Reibenspies, J. H. *Inorg. Chem.* **1999**, *38*, 2473–2481.

(29) Kristjánssdóttir, S. S.; Norton, J. R. In *Transition Metal Hydrides*; Dedieu, A., Ed.; VCH: New York, 1991; pp 309–359.

(27) Ayllon, J. A.; Sayers, S. F.; Sabo-Etienne, S.; Donnadieu, B.; Chaudret, B.; Clot, E. *Organometallics* **1999**, *18*, 3981–3990.

Table 3. Summary of Cyclic Voltammetry Data

compd	$E_{1/2}(\text{II/I})^a$	$E_{1/2}(\text{I/0})^a$
[Ni(depp) ₂](BF ₄) ₂	-0.61 (74)	-1.34 (71)
	[-0.58] (82)	[-1.34] (86)
[Ni(PNP) ₂](BF ₄) ₂	-0.64 (80)	-1.24 (66)
	[-0.60] (61)	[-1.24] (60)
[Ni(PNBuP) ₂](BF ₄) ₂	-0.63 (73)	-1.29 (70)
	[-0.60] (90)	[-1.28] (90)
[Ni(PNP)(dmpm)](BF ₄) ₂	-1.22 (195)	-1.31 (80)
Ni(dpyp) ₂	-0.80	-0.85 (61)
[HNi(depp) ₂](PF ₆)	0.00 (E_p)	
[HNi(PNP) ₂](PF ₆)	-0.62 (110)	

^a All potentials are given in volts vs the ferrocene/ferrocenium couple. Peak-to-peak separations are shown in parentheses in millivolts. Potentials not in brackets were obtained on 1×10^{-3} M solutions of the complexes in 0.2 N NEt₄BF₄ acetonitrile. Potentials shown in brackets are for 0.2 N NBu₄BF₄ benzonitrile solutions.

These electron-transfer processes are diffusion controlled, as indicated by a linear dependence of the peak currents on the square root of the scan rate.^{30a} Data for [Ni(depp)₂](BF₄)₂ and [Ni(PNP)₂](BF₄)₂ are summarized in Table 3. It is likely that the reversible or quasireversible Ni(II/I) couples of these complexes involve cleavage of weak (1–2.5 kcal/mol) Ni–acetonitrile bonds as discussed previously for related [Ni(diphosphine)₂]²⁺ complexes.²² Similar data were obtained for the Ni(0) analogues of these two complexes in benzonitrile (in which these two neutral complexes are soluble) and for Ni(dpyp)₂ and [Ni(PNP)(dmpm)](BF₄)₂ in acetonitrile (see Table 3).

The cyclic voltammogram of [HNi(depp)₂](PF₆) (trace a of Figure 3) consists of an irreversible wave with a peak potential at 0.00 V versus ferrocene at a scan rate of 50 mV/s. This wave is assigned to two overlapping one-electron oxidations. The peak height of this wave is 2.0 times that of the waves observed for the Ni(II/I) and Ni(I/0) couples of [Ni(depp)₂](BF₄)₂, and $E_p - E_{p/2}$ (the peak potential minus the peak potential at half-height) is 70 mV. Similarly, the ratio of the slopes of Q versus $t^{1/2}$ (charge vs the square root of time) plots of chronoamperometric experiments in which the potentials are stepped across the oxidation wave of [HNi(depp)₂](PF₆) and the Ni(II/I) wave of [Ni(depp)₂](BF₄)₂ is 2.1.^{30b} Scan rate studies of the anodic wave at 0.00 V indicate a diffusion-controlled process. Associated with this anodic wave are three small cathodic waves at -0.62, -0.96, and -1.34 V. The two waves at -0.62 and -1.34 V can be assigned to the Ni(II/I) and Ni(I/0) couples of [Ni(depp)₂]²⁺. The presence of these waves indicates that oxidation of [HNi(depp)₂]⁺ is followed by proton loss and formation of [Ni(depp)₂]²⁺. These data are consistent with either an EEC or an ECE process in which the chemical step is the loss of a proton.

The small cathodic wave at -0.96 V in trace a of Figure 3 is assigned to [Ni(depp)(CH₃CN)₄]²⁺. When an acetonitrile solution of [Ni(CH₃CN)₆](BF₄)₂ is titrated with depp, the peak current for this wave reaches a maximum at a 1.2:1 ratio of depp to [Ni(CH₃CN)₆](BF₄)₂ and disappears com-

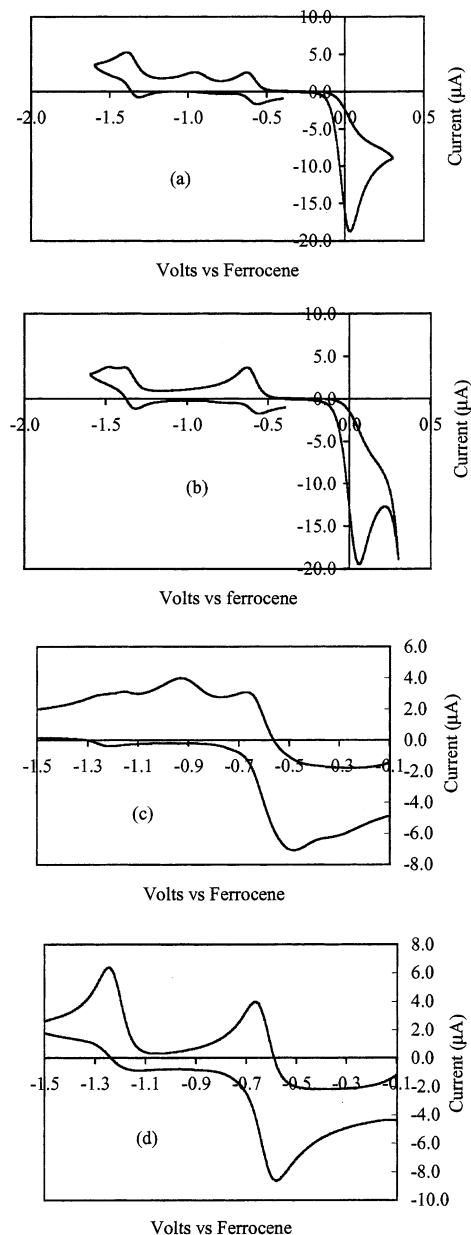


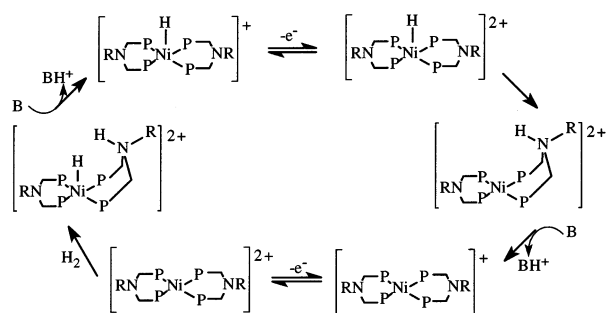
Figure 3. (a) Cyclic voltammogram of a 2.3×10^{-3} M solution of [HNi(depp)₂](PF₆) in 0.2 M NEt₄BF₄/CH₃CN. The scan rate is 100 mV/s. (b) Trace recorded after addition of triethylamine to produce a 2.5×10^{-3} M solution. (c) Cyclic voltammogram of a 1.6×10^{-3} M solution of [HNi(PNP)₂](PF₆) in 0.2 M NEt₄BF₄/CH₃CN. The scan rate is 100 mV/s. (d) Trace recorded after addition of triethylamine to produce a 2.5×10^{-3} M solution.

pletely when a 2:1 ratio is reached. These results are similar to those described previously for the titration of [Ni(CH₃CN)₆](ClO₄)₂ with PPh₃, which forms [Ni(PPh₃)₂-(CH₃CN)₄]²⁺.³¹ Titration of [Ni(depp)₂](BF₄)₂ in acetonitrile with HBF₄ also results in the appearance of a wave at -0.96 V, which reaches a maximum at a 2:1 ratio of HBF₄ to [Ni(depp)₂](BF₄)₂ (Figure 2s of Supporting Information). This wave is also observed when acetonitrile solutions of [Ni(depp)₂]²⁺ are purged with hydrogen, as expected on the basis of reaction 3. Control experiments run with protonated

(30) (a) Bard, A. J.; Faulkner, L. R. *Electrochemical Methods*; John Wiley & Sons: New York, 1980; p 218. (b) Bard, A. J.; Faulkner, L. R. *Electrochemical Methods*; John Wiley & Sons: New York, 1980; pp 201–204.

(31) Bontempelli, G.; Magno, F.; Schiavon, G.; Corain, B. *Inorg. Chem.* **1981**, *20*, 2579–2590.

Scheme 1



depp, $[\text{Ni}(\text{CH}_3\text{CN})_6](\text{BF}_4)_2$, $[\text{Ni}(\text{CH}_3\text{CN})_6](\text{BF}_4)_2$ and HBF_4 , and HBF_4 rule out the possibility of these species or a combination of these species producing the wave at -0.96 V. This wave disappears if triethylamine is added to a solution of $[\text{HNi}(\text{depp})_2](\text{PF}_6)$, trace b of Figure 3. In this case, triethylamine acts as a base toward the proton liberated upon the two-electron oxidation of $[\text{HNi}(\text{depp})_2]^+$, and the depp ligand remains bound to Ni rather than dissociating and reacting with H^+ in solution to form $[\text{Ni}(\text{depp})(\text{CH}_3\text{CN})_4]^{2+}$ and $\text{H}_2\text{depp}^{2+}$. These results are consistent with the ^1H and ^{31}P NMR spectral results already discussed for the reaction of $[\text{Ni}(\text{depp})_2]^{2+}$ with hydrogen (see reaction 3 and associated discussion).

The cyclic voltammogram of $[\text{HNi}(\text{PNP})_2](\text{PF}_6)$ shown in trace c of Figure 3 contains both similarities and differences from that observed for $[\text{HNi}(\text{depp})_2](\text{PF}_6)$. The oxidation wave of $[\text{HNi}(\text{PNMeP})_2](\text{PF}_6)$ is much more negative, -0.60 V versus 0.00 V, and the wave is now quasireversible. The peak-to-peak separation for this wave at a scan rate of 100 mV/s is 150 mV, and the ratio of the peak cathodic current to the peak anodic current is 0.75 . The anodic portion of this wave is assigned to a two-electron process. The slope for the Q versus $t^{1/2}$ plot for a potential step across the oxidation wave of $[\text{HNi}(\text{PNP})_2]^+$ is 1.0 times that of the slope for the Q versus $t^{1/2}$ plot for a potential step across both reduction waves of $[\text{Ni}(\text{PNP})_2]^{2+}$. Associated with this anodic wave are two smaller cathodic waves at -0.93 and -1.14 V. The latter wave is assigned to the Ni(I/0) couple of $[\text{Ni}(\text{PNP})_2]^{2+}$ that is shifted because of a rapid protonation of the Ni(0) complex. The small cathodic wave observed at -0.93 is assigned to a small amount of $[\text{Ni}(\text{PNP})(\text{CH}_3\text{CN})_4]^{2+}$. This product is formed in a reaction similar to the reaction observed following oxidation of $[\text{HNi}(\text{depp})_2]^+$. When triethylamine is added to an acetonitrile solution of $[\text{HNi}(\text{PNP})_2]^{2+}$, the cyclic voltammogram shown by trace d of Figure 3 is observed. Compared to trace c, the oxidation wave is sharper, and two reduction waves are observed that correspond to the (II/I) and (I/0) couples of $[\text{Ni}(\text{PNP})_2]^{2+}$. The wave assigned to the reduction of $[\text{Ni}(\text{PNP})(\text{CH}_3\text{CN})_4]^{2+}$ is absent.

These results are consistent with the reactions shown in Scheme 1. The one-electron oxidation of $[\text{HNi}^{\text{III}}(\text{PNP})_2]^+$ to $[\text{HNi}^{\text{IV}}(\text{PNP})_2]^{2+}$ is followed by rapid transfer of the proton bound to Ni in $[\text{HNi}^{\text{III}}(\text{PNP})_2]^+$ to the N atom of the chelating PNP ligand. In the presence of triethylamine, a proton transfer occurs from the diphosphine ligand to give

$[\text{Ni}^{\text{I}}(\text{PNP})_2]^+$ and HNEt_3^+ . Oxidation of $[\text{Ni}^{\text{I}}(\text{PNP})_2]^+$ to $[\text{Ni}^{\text{II}}(\text{PNP})_2]^{2+}$ completes the two-electron oxidation process. The potential of the oxidation wave of $[\text{HNi}^{\text{III}}(\text{PNP})_2]^+$ ($E_{1/2} = -0.62$ V) coincides with that of the (II/I) couple of $[\text{Ni}(\text{PNP})_2]^{2+}$ ($E_{1/2} = -0.64$ V). The latter species is reduced in two waves as expected upon reversal of the scan direction. In the absence of triethylamine, oxidation of $[\text{HNi}^{\text{III}}(\text{PNP})_2]^+$ is presumably still followed by proton migration to form $[\text{Ni}^{\text{I}}(\text{PNP})(\text{PNHP})]^{2+}$. However, this species in the absence of a base can undergo proton exchange with itself to form the doubly N-protonated species, $[\text{Ni}^{\text{I}}(\text{PNHP})_2]^{3+}$, and the unprotonated species, $[\text{Ni}^{\text{I}}(\text{PNP})_2]^+$. This following reaction could account for species that lead to the observed shoulders on the oxidation wave at -0.60 V (trace c of Figure 3). The observation that these shoulders collapse to a single oxidation wave in the presence of a triethylamine is consistent with different protonated versions of $[\text{Ni}^{\text{I}}(\text{PNP})_2]^+$.

Because $[\text{Ni}^{\text{III}}(\text{depp})_2]^{2+}$ and $[\text{Ni}^{\text{III}}(\text{PNP})_2]^{2+}$ react rapidly with hydrogen on a preparative scale (i.e., minutes), bulk electrolysis experiments were performed on acetonitrile solutions of $[\text{Ni}(\text{PNP})_2]^{2+}$ under 1 atm of H_2 in the presence of triethylamine. When a potential sufficient to oxidize $[\text{HNi}(\text{PNP})_2]^+$ was applied for 6 h, 15 mol of H^+ were generated for each mole of catalyst. This experiment confirms the catalytic nature of $[\text{Ni}(\text{PNP})_2]^{2+}$ for electrochemical hydrogen oxidation, but no attempt was made to exhaustively oxidize hydrogen until the catalyst was deactivated. Cyclic voltammograms of $\text{Ni}^{\text{0}}(\text{depp})_2$ and $\text{Ni}^{\text{0}}(\text{PNP})_2$ were recorded in benzonitrile under hydrogen in the presence and absence of triethylamine. No enhanced current was observed for the $\text{Ni}^{\text{III}}/\text{Ni}^{\text{0}}$ oxidation waves. The failure to observe a catalytic wave for $\text{Ni}^{\text{0}}(\text{PNP})_2$ is attributed to the slow activation of hydrogen on the cyclic voltammetry time scale (i.e., a second order rate constant less than approximately $100 \text{ M}^{-1} \text{ s}^{-1}$) by $[\text{Ni}^{\text{III}}(\text{PNP})_2]^{2+}$. An alternative possibility is that the transfer of protons is slow, but as discussed, the transfer of a proton from Ni to a bridging N atom and then to a base in solution is rapid on NMR and cyclic voltammetry time scales. For these reasons, we conclude that the slowness of the reaction of $[\text{Ni}(\text{PNP})_2]^{2+}$ with hydrogen is the reason for not observing a catalytic response by cyclic voltammetry. However, reaction with hydrogen is still relatively fast, with complete conversion of $[\text{Ni}(\text{PNP})_2]^{2+}$ to $[\text{HNi}(\text{PNP})(\text{PNHP})]^{2+}$ in less than 2 min from the time of hydrogen addition, if mixing is vigorous.

Discussion

Design and Synthesis of Complexes. Previous studies have shown that $[\text{Ni}(\text{diphosphine})_2]^{2+}$ complexes can act as hydride acceptors in the presence of suitable bases.¹⁹ Our objective was to extend these studies to incorporate both hydride and proton acceptor sites in the same molecule. This led to our attempts to prepare $[\text{Ni}(\text{diphosphine})_2]^{2+}$ complexes containing 1,2-bis(di-2-pyridylphosphino)ethane²⁴ as a ligand. This ligand contains pendant terminal pyridyl substituents that could act as an internal base, and ruthenium complexes of this type have been used to catalyze the hydrogenation of imines.³² However, when this ligand was

Functional Model for Hydrogenases

reacted with $[\text{Ni}(\text{CH}_3\text{CN})_6](\text{BF}_4)_2$, no ^{31}P NMR resonances were observed, and resonances in the ^1H NMR spectrum were extremely broad. This was attributed to the formation of a paramagnetic species, which is inconsistent with a square planar $[\text{Ni}(\text{diphosphine})_2]^{2+}$ complex. To promote the formation of Ni–P bonds, the softer Ni(0) complex, $\text{Ni}(\text{COD})_2$, was reacted with dpype to form $\text{Ni}(\text{dpype})_2$. In this case, the phosphorus atoms are coordinated to Ni, as shown in Figure 1c. Oxidation of $\text{Ni}(\text{dpype})_2$ with 2 equiv of ferrocenium hexafluorophosphate produced a paramagnetic product or products, again inconsistent with the formation of the desired diamagnetic square planar complex with four coordinated phosphorus atoms.

To overcome the problems encountered with dpype, the PNP and PNBuP ligands were prepared to favor coordination of P atoms over N atoms. For these ligands, there are fewer N atoms to coordinate to Ni, and the four-membered chelate rings resulting from coordination of nitrogen and phosphorus should be less favorable than the six-membered rings that result from coordination of PNP through the phosphorus atoms. Using the PNP ligand, $[\text{Ni}(\text{PNP})_2](\text{BF}_4)_2$, $[\text{Ni}(\text{PNP})(\text{dmpm})](\text{BF}_4)_2$, $[\text{HNi}(\text{PNP})_2](\text{PF}_6)_2$, and $\text{Ni}(\text{PNP})_2$ complexes can be prepared as described. All of these complexes contain PNP ligands coordinated through the two phosphorus atoms, whereas the N atoms function as pendant bases and do not coordinate to Ni.

Factors Affecting the Heterolytic Cleavage of Hydrogen. The cations $[\text{Ni}(\text{PNP})_2]^{2+}$ and $[\text{Ni}(\text{PNP})(\text{dmpm})]^{2+}$ contain hydride acceptor sites, the Ni atoms, and proton acceptor sites, the N atoms of the PNP ligands. However, only $[\text{Ni}(\text{PNP})_2]^{2+}$ reacts with 1 atm of hydrogen at room temperature. The free energy associated with this heterolytic cleavage reaction can be evaluated using the thermodynamic cycle shown in reactions 7–10. Reaction 7 is the heterolytic cleavage of hydrogen in acetonitrile. The free energy for this reaction is 76 kcal/mol.^{19,33} The hydride donor ability of $[\text{HNi}(\text{PNP})_2]^+$ (the reverse of reaction 8) is 66 kcal/mol, as already discussed. Finally, the $\text{p}K_a$ of $[\text{HNi}(\text{PNP})(\text{PNHP})]^{2+}$ is 10.6, which gives a free energy of -15 kcal/mol ($\Delta G^\circ_9 = -1.37\text{p}K_a$) for reaction 9. The sum of these reactions is the heterolytic cleavage of hydrogen by $[\text{Ni}(\text{PNP})_2]^{2+}$, reaction 10, with a corresponding free energy of -5 kcal/mol. This result indicates that hydrogen activation by $[\text{Ni}(\text{PNP})_2]^{2+}$ should be thermodynamically favored, as observed.

For $[\text{Ni}(\text{PNP})(\text{dmpm})]^{2+}$, a hydride acceptor ability of -55 kcal/mol can be calculated using a linear relationship that exists between the hydride acceptor ability of $[\text{Ni}(\text{diphosphine})_2]^{2+}$ complexes and the $\text{Ni}^{(\text{II/I})}$ couple for these complexes.²⁵ This estimate is expected to be accurate within ± 2 kcal/mol. Similarly, the $\text{p}K_a$ of $[\text{HNi}(\text{PNHP})(\text{dmpm})]^{2+}$ is taken to be 10.6, the same as that measured for $[\text{HNi}(\text{PNP})(\text{PNHP})]^{2+}$. It is not anticipated that the acidity of the PNHP⁺ ligand will differ significantly for these two complexes.

Using the cycle shown by reactions 7–10, a hydride acceptor ability of -55 kcal/mol for $[\text{Ni}(\text{PNP})(\text{dmpm})]^{2+}$, and a $\text{p}K_a$ of 10.6 for $[\text{HNi}(\text{PNHP})(\text{dmpm})]^{2+}$ gives a free energy of $+6$ kcal/mol for the heterolytic cleavage of hydrogen by $[\text{Ni}(\text{PNP})(\text{dmpm})]^{2+}$. The free energies calculated for the heterolytic cleavage of hydrogen by $[\text{Ni}(\text{PNP})_2]^{2+}$ (-5 kcal/mol) and $[\text{Ni}(\text{PNP})(\text{dmpm})]^{2+}$ ($+6$ kcal/mol) provide an explanation for the observed differences in reactivity of these two complexes.

	ΔG° (kcal/mol)	
$\text{H}_{2(\text{g})} \rightarrow \text{H}^+(\text{s}) + \text{H}^-(\text{s})$	76	(7)
$[\text{Ni}(\text{PNP})_2]^{2+} + \text{H}^- \rightarrow [\text{HNi}(\text{PNP})_2]^+$	-66	(8)
$[\text{HNi}(\text{PNP})_2]^+ + \text{H}^+ \rightarrow [\text{HNi}(\text{PNP})(\text{PNHP})]^{2+}$	-15	(9)
$\text{H}_{2(\text{g})} + [\text{Ni}(\text{PNP})_2]^{2+} \rightarrow [\text{HNi}(\text{PNP})(\text{PNHP})]^{2+}$	-5	(10)

The greater hydride acceptor ability of $[\text{Ni}(\text{PNP})_2]^{2+}$ compared to $[\text{Ni}(\text{PNP})(\text{dmpm})]^{2+}$ is attributed to the larger tetrahedral distortion of this complex. It has been shown for $[\text{Ni}(\text{diphosphine})_2]^{2+}$ complexes that both the hydride acceptor ability and the potential of the $\text{Ni}^{(\text{II/I})}$ couple are strongly affected by the chelate bite size of the diphosphine ligand.^{19,22} These effects can, in turn, be traced to a tetrahedral distortion of these nominally square planar complexes.^{21,22} As seen in the structures of $[\text{Ni}(\text{PNBuP})_2]^{2+}$ and $[\text{Ni}(\text{PNP})(\text{dmpm})]^{2+}$ (Figure 1), the former has a large tetrahedral distortion whereas the latter is nearly planar. This tetrahedral distortion results in a much lower energy for the acceptor orbital for the hydride ligand, and hence, $[\text{Ni}(\text{PNBuP})_2]^{2+}$ and $[\text{Ni}(\text{PNP})_2]^{2+}$ are better hydride acceptors than $[\text{Ni}(\text{PNP})(\text{dmpm})]^{2+}$. The large tetrahedral distortions observed about Ni in the NiFe hydrogenases^{12–14} are likely to have the same effects. That is, the $\text{Ni}^{(\text{II/I})}$ couple is expected to be more positive, and the $\text{Ni}^{(\text{II})}$ form should be a better hydride acceptor than would be observed for a more planar structure.

The Fe-only form of the enzyme is attached to the protein at only one point, a bridging cysteine. As a result, the geometry of the active site may not be strongly influenced by the protein structure. However, for the Ni/Fe hydrogenases, the Ni sites are bound to four cysteine S atoms and have large tetrahedral distortions.^{12–14} In comparison, the CO dehydrogenase enzyme of *Carboxydotherrmus hydrogeniformans* contains a Ni bound to four sulfur atoms, but in this case, the Ni atom lies in a nearly square planar environment.³⁴ It is clear that the protein can exert a strong influence on the geometry about Ni, and this geometry plays a major role in the energetics of heterolytic activation of hydrogen in model compounds and in their observed redox potentials. This is consistent with an important role of protein structure not only in positioning multiple binding sites for substrates but also in modulating the activity of active sites by controlling the geometry of the coordination sphere of metal ions.

(32) Jones, N. D.; MacFarlane, K. S.; Smith, M. B.; Schutte, R. P.; Rettig, S. J.; James, B. R. *Inorg. Chem.* **1999**, *38*, 3956–3966.

(33) Wayner, D. D. M.; Parker, V. D. *Acc. Chem. Res.* **1993**, *26*, 287–294.

(34) Dobbek, H.; Svetlitchnyi, V.; Gremer, L.; Huber, R.; Meyer, O. *Science* **2001**, *293*, 1281–1285.

Intra- and Intermolecular H/D Exchange. The heterolytic cleavage of hydrogen by $[\text{Ni}(\text{PNP})_2]^{2+}$ results in a hydride ligand on Ni and a proton on a bridging N atom of the diphosphine ligand. As discussed, the NH proton and the hydride ligand of $[\text{HNi}(\text{PNHP})(\text{PNP})]^{2+}$ exchange rapidly on the NMR time scale. This is consistent with the formation of an intermediate dihydrogen or dihydride complex resulting from the transfer of the proton from N to the hydride ligand or to Ni (reactions 5 or 6) and probably occurs when the PNP ligand is in the boat form. Rapid rotation followed by cleavage of the dihydrogen ligand by the N of the diphosphine ligand to reform the NH bond, or transfer of the second hydride ligand of the dihydride, would provide reasonable explanations for the observed exchange. Both the hydride ligand and the NH proton exchange rapidly with protons in solution, as discussed. The exchange of the hydride ligand occurs by exchange of the NH proton of the ligand with proton sources in solution (possibly when the PNP ligand is in the chair form), followed by the rapid intramolecular exchange between the NH proton and the hydride. The hydride ligand of $[\text{HNi}(\text{PNP})_2]^+$ also exchanges rapidly with the deuterium nuclei of D_2O , as indicated by the exchange experiments already discussed. This reaction likely proceeds in a similar fashion, that is, protonation of the N atom of one of the diphosphine ligands followed by exchange with the hydride ligand. In contrast, no rapid proton exchange is observed between D_2O and the hydride of $[\text{HNi}(\text{depp})_2]^{2+}$, which is structurally very similar but does not have a bridging N atom in the backbone of the ligand. As a result, for $[\text{HNi}(\text{depp})_2]^{2+}$, exchange must occur directly between the hydride ligand on Ni and the proton source in solution. This is a much slower process requiring several days. Complexes containing NH and OH protons and hydridic functional groups have generally shown rapid exchange of the NH or OH proton with water, but the intramolecular exchange of these protons with the metal hydride can be slow or fast.^{10,26} The role played by the bridging N atom of the PNP ligand in the proton exchange processes described for $[\text{HNi}(\text{PNP})_2](\text{PF}_6)$ and $[\text{HNi}(\text{PNP})(\text{PNHP})](\text{BF}_4)_2$ is the same as that proposed for the bridging di(thiomethyl)amine ligand in the Fe-only hydrogenases.¹

Role of the Bridging N Atom in the Oxidation of $[\text{HNi}(\text{PNP})_2]^+$. The electrochemical reduction of the Ni^{III} complexes, $[\text{Ni}(\text{depp})_2]^{2+}$ and $[\text{Ni}(\text{PNP})_2]^{2+}$, are remarkably similar, both exhibiting two reversible one-electron reductions at nearly the same potentials. However, the oxidations of the corresponding Ni–H complexes, $[\text{HNi}(\text{PNP})_2]^+$ and $[\text{HNi}(\text{depp})_2]^+$, are quite different. The oxidation of the former occurs at a potential that is approximately 0.6 V negative of the potential observed for the latter. The only major difference between these two complexes is the presence of a N atom in the chelate ring of the ligand of one and not the other. This difference in potentials is consistent with a rapid proton transfer from Ni to the N atom and ultimately to the solution. A rapid proton transfer from Ni to N implies that the $\text{p}K_{\text{a}}$ values of $[\text{Ni}^{\text{II}}(\text{PNHP})(\text{PNP})]^{2+}$ should be nearly equal to or larger than that of its isomeric form, $[\text{HNi}^{\text{III}}(\text{PNP})_2]^{2+}$, to avoid a large activation barrier.

Although Ni^{II} and Ni^{III} complexes have not been isolated in this work, we estimate the $\text{p}K_{\text{a}}$ values of the pendant NH of $[\text{Ni}^{\text{II}}(\text{PNP})(\text{PNHP})]^{2+}$ to be between the measured $\text{p}K_{\text{a}}$ of 8.7 for $[\text{Ni}^{\text{III}}(\text{PNHP})(\text{dmpm})]^{3+}$ and 10.6 for $[\text{HNi}^{\text{III}}(\text{PNP})(\text{PNHP})]^{2+}$. $[\text{Ni}^{\text{II}}(\text{PNP})(\text{PNHP})]^{2+}$ has a lower positive charge than $[\text{Ni}^{\text{III}}(\text{PNHP})(\text{dmpm})]^{3+}$. This should result in $[\text{Ni}^{\text{II}}(\text{PNP})(\text{PNHP})]^{2+}$ having a larger $\text{p}K_{\text{a}}$ than $[\text{Ni}^{\text{III}}(\text{PNHP})(\text{dmpm})]^{3+}$. However, $[\text{Ni}^{\text{II}}(\text{PNP})(\text{PNHP})]^{2+}$ lacks the possibility for hydrogen-bond formation between the NiH and the NH proton that is possible in $[\text{HNi}^{\text{III}}(\text{PNP})(\text{PNHP})]^{2+}$. As a result, it is anticipated that the $\text{p}K_{\text{a}}$ of $[\text{Ni}^{\text{II}}(\text{PNP})(\text{PNHP})]^{2+}$ should be less than, or equal to, that of $[\text{HNi}^{\text{III}}(\text{PNP})(\text{PNHP})]^{2+}$.

The $\text{p}K_{\text{a}}$ of $[\text{HNi}^{\text{III}}(\text{PNP})_2]^{2+}$ is estimated to be 7.7 ± 2.5 . This value was calculated using the $\text{p}K_{\text{a}}$ value of 22.2 measured for $[\text{HNi}^{\text{III}}(\text{PNP})_2]^+$ and an estimated decrease in the $\text{p}K_{\text{a}}$ value by 14.5 $\text{p}K_{\text{a}}$ units upon oxidation to $[\text{HNi}^{\text{III}}(\text{PNP})_2]^{2+}$. The estimated decrease in the $\text{p}K_{\text{a}}$ value is based on the observation that the $\text{p}K_{\text{a}}$ of the isoelectronic hydride, $\text{HCo}^{\text{I}}(\text{dppe})_2$, decreases by 14.5 $\text{p}K_{\text{a}}$ units upon oxidation.³⁵ If a similar decrease occurs when $[\text{HNi}^{\text{II}}(\text{PNP})_2]^+$ is oxidized to $[\text{HNi}^{\text{III}}(\text{PNP})_2]^{2+}$, a $\text{p}K_{\text{a}}$ value of 7.7 should be reasonable. A similar $\text{p}K_{\text{a}}$ value of 9.3 has been reported for $[\text{HNi}^{\text{III}}(\text{cyclam})]^+$ (where cyclam is 1,4,8,11-tetraazacyclotetradecane).³⁶ These estimated $\text{p}K_{\text{a}}$ values indicate that the transfer of the proton from the Ni atom to the N atom of $[\text{HNi}^{\text{III}}(\text{PNP})_2]^{2+}$ should be favorable by 1–2 $\text{p}K_{\text{a}}$ units. On this basis, it is reasonable that oxidation of $[\text{HNi}(\text{PNP})_2]^+$ to $[\text{HNi}(\text{PNP})_2]^{2+}$ would be followed by rapid proton transfer to form $[\text{Ni}(\text{PNHP})(\text{PNP})]^{2+}$. Subsequent deprotonation of the latter complex by a base in solution results in the formation $[\text{Ni}(\text{PNP})_2]^+$ which reoxidizes to $[\text{Ni}(\text{PNP})_2]^{2+}$ at -0.64 V. This completes a cycle for hydrogen oxidation that involves two important proton-transfer steps mediated by the PNP ligand. A similar role has been proposed for the di(thiomethyl)amine in Fe-only hydrogenases.¹

Summary

The complex $[\text{Ni}(\text{PNP})_2](\text{BF}_4)_2$ incorporates both hydride and proton acceptor sites in a single metal complex. Comparison of $[\text{Ni}(\text{PNP})_2](\text{BF}_4)_2$, $\text{Ni}(\text{PNP})_2$, and $[\text{HNi}(\text{PNP})_2](\text{PF}_6)$ with analogous Ni complexes of depp in which the bridging N has been replaced with a methylene group confirms the important role of the pendant N base in hydrogen activation and proton-transfer processes. $[\text{Ni}(\text{PNP})_2](\text{BF}_4)_2$ exhibits many of the features of hydrogenase enzymes. Heterolytic activation of hydrogen by this complex is observed with the formation of a NiH site ($\Delta G_{\text{H}^-}^\circ = 66$ kcal/mol) and a protonated N atom of the pendant base on one diphosphine ligand ($\text{p}K_{\text{a}} = 10.6$). This reaction is similar to the first step proposed in the activation of H_2 by Fe-only hydrogenases. Comparison of the molecular structures of

(35) Ciancanelli, R.; Noll, B. C.; DuBois, D. L.; DuBois, M. R. *J. Am. Chem. Soc.* **2002**, *124*, 2984–2992.

(36) Kelly, C. A.; Mulazzani, Q. G.; Venturi, M.; Blinn, E. L.; Rodgers, M. A. *J. Am. Chem. Soc.* **1995**, *117*, 4911–4919. These authors report a $\text{p}K_{\text{a}}$ value of 1.8 in water. This value has been converted to an acetonitrile value by adding 7.5 $\text{p}K_{\text{a}}$ units as suggested in ref 29.

[Ni(PNBuP)₂](BF₄)₂ and [Ni(PNP)(dmpm)](BF₄)₂ and their reactions with hydrogen illustrates that the larger tetrahedral distortion observed for [Ni(PNBuP)₂](BF₄)₂ increases the hydride acceptor ability of the Ni site by about 10 kcal/mol. The NH and NiH protons of [HNi(PNP)(PNHP)]²⁺, the product of heterolytic cleavage of hydrogen by [Ni(PNP)₂]²⁺, undergo rapid intramolecular exchange (~10⁴ s⁻¹), and both sites undergo rapid proton exchange with protonated bases in solution. Treatment of [HNi(PNP)(PNHP)]²⁺ with bases whose protonated forms have pK_a values greater than 10.6 results in the formation of [HNi(PNP)₂]⁺. Oxidation of the latter hydride at the electrode results in a rapid proton transfer from the resulting Ni^(III)H to the N atom of a PNP ligand to form [Ni^(II)(PNHP)(PNP)]²⁺ with an estimated driving force of 1–4 kcal/mol. This rapid proton transfer between Ni and N results in a 0.6 V decrease in the oxidation potential of [HNi(PNP)₂]⁺ compared to [HNi(depp)₂]⁺ and a much more reversible process. Subsequent transfer of a proton from the (PNHP)⁺ ligand of [Ni^(II)(PNHP)(PNP)]²⁺ (pK_a 8.7–10.6) to a base in solution results in the formation of [Ni^(II)(PNP)₂]⁺ which can be reoxidized (–0.64 V) to form the original Ni(II) complex. This catalytic cycle involves extensive participation of the pendant base of the PNP ligand in a number of proton transfer steps. Similar interactions between the di-(thiomethyl)amine ligand and the active Fe sites of the Fe-only hydrogenases may contribute significantly to their catalytic activity and redox properties.

Experimental Section

Spectral and Electrochemical Measurements. ¹H NMR and ³¹P NMR spectra were recorded on a Varian Unity 300 MHz spectrometer. ¹H chemical shifts are reported relative to tetramethylsilane using residual solvent protons as a secondary reference. ¹H NMR spectra in benzonitrile were recorded on a Varian Inova 400 spectrometer with solvent suppression using the Varian WET1d pulse sequence. ³¹P NMR spectra were proton decoupled and referenced to external phosphoric acid. Infrared spectra of Nujol mulls were recorded on a Nicolet 510P spectrometer.

All electrochemical experiments were carried out under an atmosphere of N₂ in 0.2 M Et₄NBF₄ acetonitrile solutions or 0.2 M Bu₄NBF₄ benzonitrile solutions. Cyclic voltammetry and chronoamperometric studies were carried out on a Cypress Systems computer aided electrolysis system. The working electrode was a glassy carbon disk, the counter electrode was a glassy carbon rod, and the reference electrode was a silver wire immersed in a permethylferrocene/permethylferrocenium solution. Ferrocene was used as an internal standard, and all potentials are referenced to the ferrocene/ferrocenium couple.

Syntheses and Materials. All reactions were performed using standard Schlenk techniques under nitrogen, and all solvents were purified using standard procedures. All commercially available materials were of reagent-grade, or higher, quality. [Ni(CH₃CN)₆]-[BF₄]₂,³⁷ [Ni(depp)₂](BF₄)₂,¹⁹ [HNi(depp)₂](PF₆)₂,¹⁹ and dpype²⁴ were prepared according to literature methods.

PNP, Bis(diethylphosphinomethyl)methylamine. A Schlenk flask was charged with diethylphosphine (2.27 g, 25.2 mmol) and degassed aqueous formaldehyde (37 wt %, 1.95 mL, 26 mmol) in ethanol (10 mL). After stirring for 30 min, the hydrochloride salt

of methylamine (CH₃NH₂Cl, 0.85 g, 12.65 mmol) was added as an ethanol/water solution (10 mL, 3:1 ratio), followed by triethylamine (2 mL, 14 mmol). The mixture was stirred at room temperature for 3 h, and the solvent was removed in vacuo. The product was extracted with diethyl ether (3 × 25 mL). Removal of the solvent from the combined extracts produced a clear liquid (2.12 g, 71% yield). Anal. Calcd for C₁₁H₂₇P₂N: C, 56.15; H, 11.57; N, 5.95; P, 26.33. Found: C, 55.73; H, 12.22; N, 5.78; P, 25.76. ¹H NMR (CD₃CN): 2.62 ppm (d, ²J_{PH} = 2.1 Hz, PCH₂N); 2.36 ppm (s, NCH₃); 1.37 ppm (q, ³J_{HH} = 7.8 Hz, PCH₂CH₃); 1.02 ppm (d of tr, ³J_{PH} = 14.1 Hz, PCH₂CH₃). ³¹P NMR (CD₃CN): –30.99 ppm (s).

Et₂PCH₂OH (Hydroxymethyl)diethylphosphine. A Schlenk flask was charged with diethylphosphine (2.50 g, 28 mmol) and degassed aqueous formaldehyde (37 wt %, 2.75 g, 30 mmol) in ethanol (10 mL). The reaction mixture was stirred overnight, and the solvent was removed with a vacuum at low temperature (0 °C) to produce a clear liquid (3.20 g, 95% yield). The product was vacuum-distilled at 39–41 °C. ¹H NMR (CD₃OD): 4.64 ppm (s, PCH₂OH); 3.84 ppm (d, ²J_{PH} = 6.9 Hz, PCH₂OH); 1.1 and 1.3–1.6 ppm (m, PCH₂CH₃). ³¹P NMR (CD₃OD): –14.95 ppm (s).

PNBuP, Bis(diethylphosphinomethyl)butylamine. A mixture of Et₂PCH₂OH (2.80 g, 23.3 mmol), *n*-butylamine (0.78 g, 10.7 mmol), ethanol (30 mL), and magnesium sulfate (5 g) was stirred overnight at room temperature. This mixture was filtered via cannula, and the solvent and excess phosphine were removed from the filtrate with a vacuum at 70 °C to yield a clear liquid (1.40 g, 47% yield). ¹H NMR (CD₃CN): 2.72 ppm (m, PCH₂N); 2.58 ppm (tr, ³J_{HH} = 6.9 Hz, NCH₂CH₂CH₂CH₃); 1.2–1.5 ppm (m, PCH₂CH₃ and NCH₂CH₂CH₂CH₃); 1.03 ppm (d of tr, ³J_{PH} = 14.4 Hz and ³J_{HH} = 5.4 Hz, PCH₂CH₃); 0.89 ppm (tr, ³J_{HH} = 7.2 Hz, NCH₂CH₂CH₂CH₃). ³¹P NMR (CD₃CN): –32.20 ppm (s).

Ni(PNP)₂. Solid Ni(COD)₂ (0.38 g, 1.38 mmol) was added to a solution of PNP (0.65 g, 2.76 mmol) in tetrahydrofuran (30 mL) that had been cooled to –80 °C. The resulting suspension was allowed to warm to room temperature while stirring. Solvent was removed from the light yellow solution with a vacuum to produce a white solid that was washed with acetonitrile (5 mL) and dried in a vacuum (0.59 g, 81%). Anal. Calcd for C₂₂H₅₄N₂P₄Ni: C, 49.93; H, 10.28; N, 5.29. Found: C, 49.15; H, 10.36; N, 4.96. ¹H NMR (toluene-*d*₈): 2.42 ppm (s, PCH₂N); 2.22 ppm (s, NCH₃); 1.31 and 1.63 ppm (m, PCH₂CH₃); 1.05 ppm (m, PCH₂CH₃). ³¹P NMR (toluene-*d*₈): 6.60 ppm (s).

[Ni(PNP)₂H](PF₆). A solution of NH₄PF₆ (0.20 g, 1.23 mmol) in ethanol (10 mL) was filtered and added to a solution of Ni(PNP)₂ (0.30 g, 0.57 mmol) in tetrahydrofuran (30 mL) at room temperature. The resulting yellow solution was stirred for 0.5 h, and the volume reduced to 10 mL. Yellow crystalline needles formed when the reaction flask was placed in a freezer overnight. These were collected by filtration and dried in a vacuum (yield 0.20 g, 51%). Anal. Calcd for C₂₂H₅₅N₂P₅F₆Ni: C, 39.13; H, 8.21; N, 4.15. Found: C, 38.05; H, 8.14; N, 4.13. ¹H NMR (CD₃CN): 2.70 ppm (s, PCH₂N); 2.38 ppm (s, NCH₃); 1.62 and 1.72 ppm (m, PCH₂CH₃); 1.06 ppm (m, PCH₂CH₃); –14.75 ppm (pentet, ²J_{PH} = 6.3 Hz, NiH). ³¹P NMR (CD₃CN): 5.46 ppm (s). IR (Nujol mull): 1933 cm⁻¹ (ν Ni–H).

[Ni(PNP)₂](BF₄)₂. Solid [Ni(CH₃CN)_{6.5}](BF₄)₂ (0.62 g, 1.25 mmol) was added to a solution of PNP (0.59 g, 2.50 mmol) in acetonitrile (30 mL), and the resulting deep red solution was stirred at room temperature for 1 h. Removal of the solvent in a vacuum resulted in a red powder (0.74 g, 74%) that was washed with hexanes (50 mL) and dried in a vacuum. Numerous attempts to recrystallize the product resulted in decomposition. Anal. Calcd

(37) Hathaway, B. J.; Holah, D. G.; Underhill, A. E. *J. Chem. Soc.* **1962**, 2444.

for $C_{22}H_{54}N_2P_4B_2F_8Ni$: C, 37.59; H, 7.74; N, 3.99. Found: C, 36.92; H, 7.69; N, 3.99. 1H NMR (CD_3CN): 2.87 ppm (s, PCH_2N); 2.44 ppm (s, NCH_3); 2.0 ppm (m, PCH_2CH_3); 1.21 ppm (m, PCH_2CH_3). ^{31}P NMR (CD_3CN): 1.70 ppm (s).

[Ni(PNBuP) $_2$](BF $_4$) $_2$. This complex can be prepared using the procedure described for [Ni(PNP) $_2$](BF $_4$) $_2$. This compound was recrystallized rapidly (approximately 30 min) from a mixture of dichloromethane and ethanol without change. Recrystallization from this solvent mixture over a period of several days resulted in red crystals of [Ni(PNBuP) $_2$](BF $_4$) $_2$, suitable for X-ray studies, and a yellow powder identified as [HNi(PNBuP) $_2$](BF $_4$) by 1H and ^{31}P NMR. 1H NMR (CD_3CN): 2.95 ppm (s, PCH_2N); 2.61 ppm (tr, $^3J_{HH} = 7.8$ Hz, $NCH_2CH_2CH_2CH_3$); 1.1–1.5 and 2.0 ppm (m, PCH_2CH_3 and $NCH_2CH_2CH_2CH_3$); 0.91 (tr, $^3J_{HH} = 7.5$ Hz, $NCH_2CH_2CH_2CH_3$). ^{31}P NMR (CD_3CN): 1.81 ppm (s).

[Ni(PNP)(dmpm)](BF $_4$) $_2$. Solid [Ni(CH $_3$ CN) $_{6.5}$](BF $_4$) $_2$ (0.50 g, 1.0 mmol) was added to a solution of PNP (0.235 g, 1.0 mmol) and bis(dimethylphosphino)methane (dmpm, 0.136 g, 1.0 mmol) in acetonitrile (50 mL). The resulting red solution was stirred for 1 h, and the solvent was removed by applying a vacuum. Recrystallization of the orange powder that formed from a dichloromethane/ethanol mixture produced crystals suitable for a single-crystal X-ray structure determination (yield 0.41 g, 68%). Anal. Calcd for $C_{16}H_{41}NP_4B_2F_8Ni$: C, 31.83; H, 6.85; N, 2.32. Found: C, 31.47; H, 6.76; N, 2.52. 1H NMR (CD_3CN): 3.21 ppm (virtual triplet, splitting = 12.0 Hz, PCH_2P); 2.78 ppm (m, PCH_2N); 2.44 ppm (m, NCH_3); 1.90 ppm (m, PCH_2CH_3); 1.70 ppm (virtual triplet, splitting = 6.3 Hz, PCH_3); 1.17 ppm (d of tr, $^3J_{HH} = 7.5$ Hz, $^3J_{PH} = 15.6$ Hz, PCH_2CH_3). ^{31}P NMR (CD_3CN): -53.42 ppm (apparent doublet, $N = 123$ Hz, dmpm); 2.25 ppm (apparent doublet, PNP).

Ni(dpype) $_2$. Solid Ni(COD) $_2$ (0.275 g, 1.0 mmol) was added to a cold (-80 °C) solution of 1,2-bis[di(2-pyridyl)phosphino]ethane, (dpype, 0.80 g, 2.0 mmol) in tetrahydrofuran (50 mL). The resulting suspension was warmed to room temperature and stirred for 48 h. During this time, a dark red solution and an orange precipitate formed. The solid (0.28 g; 32%) was collected by filtration, recrystallized from hot acetonitrile (50 mL), and dried in a vacuum. The crystals obtained were suitable for an X-ray diffraction study. Anal. Calcd for $C_{44}H_{40}N_8P_4Ni$: C, 61.21; H, 4.67; N, 12.98. Found: C, 60.31; H, 4.87; N, 12.93. 1H NMR (toluene- d_8): 6.42 ppm (tr, $J = 6.6$ Hz, PC_5H_4N); 6.71 ppm (tr, $J = 7.5$ Hz, PC_5H_4N); 7.35 ppm (d, $J = 7.5$ Hz, PC_5H_4N); 8.30 (d, $J = 3.9$ Hz, PC_5H_4N); 3.28 ppm (s, PCH_2CH_2P). ^{31}P NMR (toluene- d_8): 57.41 ppm (s).

Ni(dpype) $_2$ Oxidation with Ferrocenium. Treatment of [Ni(dpype) $_2$] with 2 equiv of Cp $_2$ FeBF $_4$ in acetonitrile- d_3 resulted in paramagnetic products with no ^{31}P NMR signal and only broad 1H NMR signals. This result is similar to those obtained from reactions of dpype with [Ni(CH $_3$ CN) $_{6.5}$](BF $_4$) $_2$.

[Ni(PNP) $_2$](BF $_4$) $_2$ Reactions with Hydrogen. In NMR tube experiments, solutions of [Ni(PNP) $_2$](BF $_4$) $_2$ in acetonitrile- d_3 or dichloromethane- d_2 were purged with hydrogen, and the reaction was followed by ^{31}P NMR and 1H NMR. The formation of [HNi(PNHP)(PNP)](BF $_4$) $_2$ is associated with a color change from deep red to yellow, and the reaction is complete within 10 min at room temperature. 1H NMR (CD_3CN) at room temperature: 3.10 ppm (broad s, PCH_2N); 2.78 ppm (br s, NCH_3); 1.82 and 1.72 ppm (m, PCH_2CH_3); 1.07 ppm (m, PCH_2CH_3); -3.35 ppm (broad s, average of Ni-H and N-H). ^{31}P NMR (CD_3CN): 7.25 ppm (s). 1H NMR (CD_2Cl_2) at room temperature: 3.18 and 2.84 ppm (broad s, PCH_2N); 2.93 and 2.52 ppm (br s, NCH_3); 2.3–1.6 ppm (m, PCH_2CH_3); 1.3–1.6 ppm (m, PCH_2CH_3); no resonance observed for Ni-H or N-H). ^{31}P NMR (CD_2Cl_2): 6.20 ppm (s). 1H NMR

(CD_2Cl_2) at -90 °C: 7.38 ppm (br s, NH); 3.7–2.3 ppm (multiple broad resonances, PCH_2N and NCH_3); 2.0–1.0 ppm (multiple broad resonances, PCH_2CH_3); -15.24 ppm (br quintet, $^2J_{PH} = 36$ Hz). ^{31}P NMR (CD_2Cl_2): 11.2, 8.5, 3.5 ppm (br multiplets). Treatment of acetonitrile- d_3 solutions containing [HNi(PNP)(PNHP)] $^{2+}$ with triethylamine (5 μ L) results in clean formation of [HNi(PNP) $_2$] $^{2+}$.

[HNi(PNHP)(PNP)] $^{2+}$ pK $_a$ Determination. Reaction of [HNi(PNP) $_2$](PF $_6$) with 1.1 equiv of 4-cyanoanilinium tetrafluoroborate or 2,5-dichloroanilinium tetrafluoroborate in CD_3CN resulted in 1H NMR and ^{31}P NMR spectra consistent with complete protonation of one N atom of the hydride complex to form [HNi(PNHP)(PNP)] $^{2+}$. 1H NMR (CD_3CN) at room temperature: 3.10 ppm (broad s, PCH_2N); 2.78 ppm (br s, NCH_3); 1.82 and 1.72 ppm (m, PCH_2CH_3); 1.07 ppm (m, PCH_2CH_3); -3.35 ppm (broad s, average of Ni-H and N-H). ^{31}P NMR (CD_3CN): 7.25 ppm (s). Reaction of [HNi(PNP) $_2$](PF $_6$) with 1.0 equiv of anisidinium tetrafluoroborate (p -CH $_3$ OC $_6$ H $_4$ NH $_2$ ·HBF $_4$) resulted in a shift of all 1H NMR and ^{31}P NMR resonances consistent with partial protonation of one N atom of the hydride complex to form [HNi(PNP)(PNHP)] $^{2+}$. Similar experiments were carried out using 5:5:1 and 10:10:1 ratios of anisidinium/anisidine/[HNi(PNP) $_2$](PF $_6$) in CD_3CN . Again, chemical shifts were consistent with rapid, reversible, and partial protonation of the bridging N atom of a PNP ligand. For experiments using a 10:10:1 ratio, the following chemical shifts were observed/ 1H NMR (CD_3CN) at room temperature: 2.76 ppm (broad s, PCH_2N); 2.44 ppm (br s, NCH_3); 1.82 and 1.72 ppm (m, PCH_2CH_3); 1.07 ppm (m, PCH_2CH_3). ^{31}P NMR (CD_3CN): 5.74 ppm (s). The equilibrium constant calculated using weighted chemical shifts for the PCH_2N , CH_3N , and phosphorus resonances for a series of four experiments was 0.19 ± 0.03 , which corresponds to a pK $_a$ value of 10.6 ± 0.3 .

[Ni(PNP)(dmpm)](BF $_4$) $_2$ Reactions with Acids. Reaction of [Ni(PNP)(dmpm)](BF $_4$) $_2$ with excess 4-cyanoanilinium tetrafluoroborate (pK $_a = 7.6$) resulted in the following chemical shifts. 1H NMR (CD_3CN) at room temperature: 3.38 ppm (broad s, PCH_2N); 3.04 ppm (br s, NCH_3). ^{31}P NMR (CD_3CN): 9.22 ppm (br d, $N = 120$ Hz, PNP); -54.1 ppm (d, dmpm). Using different ratios of 4-bromoanilinium tetrafluoroborate/4-bromoaniline/[Ni(PNP)(dmpm)](BF $_4$) $_2$ as described in the preceding experiment, a pK $_a$ value of 8.9 was obtained. A value of 8.6 was obtained using 2,5-dichloroanilinium as the acid. An average value of 8.7 ± 0.5 is taken for the pK $_a$ value.

pK $_a$ of HNi(PNP) $_2$ $^{2+}$. Ni(PNP) $_2$ (10–14 mg, 0.019–0.026 mmol) and HPt(dppe) $_2$ (PF $_6$) (22–31 mg, 0.019–0.027 mmol) were accurately weighed into each of four NMR tubes, and benzonitrile containing 10% CD_3CN (0.7 mL) was added to each. The solutions were monitored by ^{31}P and solvent suppression 1H NMR until the amounts of products and reactants present remained constant (48 h). The concentrations of HPt(dppe) $_2$ $^{2+}$ and Pt(dppe) $_2$ at equilibrium were then determined by integration of their ^{31}P resonances. The ratio [HNi(PNP) $_2$ $^{2+}$]/[HPt(dppe) $_2$ $^{2+}$] was then determined by integration of the hydride resonances in the 1H NMR, and the concentration of HNi(PNP) $_2$ $^{2+}$ was calculated using the concentration of HPt(dppe) $_2$ $^{2+}$ found in the ^{31}P spectrum. The concentration of Ni(PNP) $_2$ was then found by subtracting [HNi(PNP) $_2$ $^{2+}$] from the amount of Ni(PNP) $_2$ initially added. The equilibrium constant calculated from these four experiments was 1.6 ± 0.2 , which corresponds to a pK $_a$ value of 22.2 ± 0.1 .

[Ni(PNBuP) $_2$](BF $_4$) $_2$ Reactions with Alcohol. Addition of ethanol (50 μ L) to a solution of [Ni(PNBuP) $_2$](BF $_4$) $_2$ in acetonitrile- d_3 resulted in formation of [HNi(PNBuP) $_2$]BF $_4$ within 24 h, as indicated by ^{31}P NMR and 1H NMR spectra.

Table 4. Crystallographic and Refinement Data for [Ni(PNBuP)₂](BF₄)₂, [Ni(PNP)(dmpm)](BF₄)₂, and Ni(dpype)₂

	[Ni(PNBuP) ₂](BF ₄) ₂	[Ni(PNP)(dmpm)](BF ₄) ₂	Ni(dpype) ₂
empirical formula	C ₂₈ H ₆₆ B ₂ F ₈ N ₂ NiP ₄	C ₁₆ H ₄₁ B ₂ F ₈ NNiP ₄	C ₅₈ H ₅₆ N ₈ NiP ₄
formula mass	787.04	603.71	1047.70
cryst size, mm ³	0.26 × 0.20 × 0.20	0.48 × 0.27 × 0.27	0.31 × 0.12 × 0.09
cryst color, habit	red block	yellow needle	yellow-gold needle
crystal syst	monoclinic	orthorhombic	triclinic
space group	<i>C2/c</i>	<i>Pca2₁</i>	<i>P1</i>
<i>a</i> , Å	21.4158(12)	18.595(3)	12.134(3)
<i>b</i> , Å	9.6615(5)	9.0279(12)	13.922(2)
<i>c</i> , Å	18.8663(10)	16.339(2)	15.953(3)
α, deg	90	90	95.985(15)
β, deg	99.8340(10)	90	102.363(13)
γ, deg	90	90	99.77(2)
<i>V</i> , Å ³	3846.2(4)	2742.9(7)	2566.4(9)
<i>Z</i> , formula units/cell	4	4	2
density (calcd), Mg·m ⁻³	1.359	1.462	1.356
absorption coeff, mm ⁻¹	0.732	1.001	0.551
<i>F</i> (000)	1672	1256	1096
abs correction	semiempirical from equivalents	semiempirical from equivalents	semiempirical from equivalents
range trans coeff	0.8674 and 0.8325	0.7738 and 0.6451	0.9521 and 0.8478
<i>T</i> , K	135(2)	133(2)	143(2)
final <i>R</i> indices	<i>R</i> 1 = 0.0641	<i>R</i> 1 = 0.0482	<i>R</i> 1 = 0.0466
[<i>I</i> > 2σ(<i>I</i>)] ^a	<i>wR</i> 2 = 0.1473	<i>wR</i> 2 = 0.1174	<i>wR</i> 2 = 0.1096
reflns obsd	4000	6134	9164
<i>R</i> indices	<i>R</i> 1 = 0.0767	<i>R</i> 1 = 0.0587	<i>R</i> 1 = 0.0710
(all data)	<i>wR</i> 2 = 0.1544	<i>wR</i> 2 = 0.1277	<i>wR</i> 2 = 0.1187
GOF on <i>F</i> ² ^b	1.106	1.064	1.084

^a *R*1 = Σ||*F*_o| - |*F*_c||/Σ|*F*_o|; *wR*2 = √[Σ(*w*(*F*_o² - *F*_c²)²)/Σ(*w*(*F*_o²)²)]. ^b GOF = *S* = √[Σ(*w*(*F*_o² - *F*_c²)²)/(*M* - *N*)] where *M* is the number of reflections and *N* is the number of parameters refined.

[H₂depp](BF₄)₂. A 5-fold excess of tetrafluoroboric acid in diethyl ether was added to a solution of bis(diethylphosphino)propane (depp, ~0.1 g) in diethyl ether (20 mL). The white solid that formed was collected by filtration, washed with ether, and dried in a vacuum. ¹H NMR (CD₃CN): 5.93 ppm (d of septets, ¹*J*_{PH} = 488 Hz, (CH₂)₃(H)PEt₂⁺), 2.4–2.2 ppm (m, PCH₂-); 1.26 ppm (dt, ³*J*_{PH} = 20.7 Hz, ³*J*_{HH} = 7.2 Hz, PCH₂CH₃). ³¹P NMR (CD₃CN): 19.8 ppm (s).

Electrocatalytic Oxidation of Hydrogen with [Ni(PNP)₂]²⁺. An airtight bulk electrolysis cell with three ground glass inlets for the working, counter, and reference electrodes and two sidearms was fitted with a reticulated vitreous carbon working electrode, a tungsten wire counter electrode, and a Pt wire in an acetonitrile solution of Fe(C₅Me₅)₂/Fe(C₅Me₅)₂⁺ and 0.3 M NEt₄BF₄ as the reference electrode. The cell was charged with 15 mL of 0.3 M Et₄NBF₄ in acetonitrile and 15 mg of [Ni(PNP)₂](BF₄)₂ (0.022 mmol). The solution was purged for 15 min with hydrogen gas that was presaturated with acetonitrile. This caused the solution to turn from orange-yellow to pale yellow as expected. To the solution was added 50 μL of Et₃N (0.36 mmol) as the base. The solution was then oxidized at +100 mV (vs Fe(C₅Me₅)₂/Fe(C₅Me₅)₂⁺) for 6 h during which 32.7 C of charge were passed. This corresponds to 0.34 mmol e⁻ and thus 0.34 mmol H⁺ produced, or 15 mol of H⁺ per mol of catalyst. The acetonitrile solution from the catalysis was added to 70 mL of distilled water and stirred for 5 min. The resulting orange precipitate was removed by filtration. The colorless filtrate was titrated with 0.0798 M NaOH to the endpoint using phenolphthalein as the indicator. The titration required 4.8 mL of

NaOH solution corresponding to 0.38 mmol of OH⁻ to neutralize the acid produced, or 17 mol of H⁺ per mole of catalyst.

X-ray Diffraction Studies. Crystals were manipulated under a light hydrocarbon oil. Selected crystals were affixed with a small amount of silicone stopcock grease to thin glass fibers attached to tapered copper mounting pins. The mounted crystals were transferred to a goniometer of a Bruker SMART CCD diffractometer equipped with an LT-2a low-temperature apparatus. Crystallographic and refinement data for [Ni(PNBuP)₂](BF₄)₂, [Ni(PNP)(dmpm)](BF₄)₂, and Ni(dpype)₂ are given in Table 4. Details of data collection and structure solutions for each individual complex are provided in the Supporting Information.

Acknowledgment. This research was supported by the Director's Discretionary Research and Development program at the National Renewable Energy Laboratory and, in part, by the United States Department of Energy, Office of Basic Energy Sciences, Division of Chemical Sciences. M. Rakowski DuBois and R. Ciancanelli would like to acknowledge the support of the National Science Foundation.

Supporting Information Available: Acid titration data for [Ni(depp)₂](BF₄)₂. Complete details of the X-ray diffraction studies on Ni(dpype)₂, [Ni(PNBuP)₂](BF₄)₂, and [Ni(PNP)(dmpm)](BF₄)₂. This material is available free of charge via the Internet at <http://pubs.acs.org>.

IC020610V